8-2016

Solution based processing of garnet type oxides for optimized lithium-ion transport

Derek K. W. Schwanz
Purdue University

Graduate School Form
30 Updated 12/26/2015

PURDUE UNIVERSITY
GRADUATE SCHOOL
Thesis/Dissertation Acceptance

This is to certify that the thesis/dissertation prepared

By Derek Karl Wittenburg Schwanz

Entitled
SOLUTION BASED PROCESSING OF GARNET TYPE OXIDES FOR OPTIMIZED LITHIUM-ION TRANSPORT

For the degree of Master of Science in Materials Science Engineering ☐

Is approved by the final examining committee:

Ernesto E. Marinero
Co-chair ☐

David F. Bahr
Co-chair ☐

R. Edwin Garcia

To the best of my knowledge and as understood by the student in the Thesis/Dissertation Agreement, Publication Delay, and Certification Disclaimer (Graduate School Form 32), this thesis/dissertation adheres to the provisions of Purdue University's "Policy of Integrity in Research" and the use of copyright material.

Approved by Major Professor(s): Ernesto E. Marinero

Approved by: David F. Bahr 7/21/2016

Head of the Departmental Graduate Program Date

SOLUTION BASED PROCESSING OF GARNET TYPE OXIDES FOR OPTIMIZED LITHIUM-ION TRANSPORT

A Thesis

Submitted to the Faculty

of

Purdue University

by

Derek K. W. Schwanz

In Partial Fulfillment of the

Requirements for the Degree

of

Master of Science in Materials Science Engineering

August 2016

Purdue University

West Lafayette, Indiana

TABLE OF CONTENTS

Page

LIST OF TABLES

LIST OF FIGURES

Figure Page

ABSTRACT

Schwanz, Derek K.W. M.S.M.S.E., Purdue University, August 2016. Solution Based Processing of Garnet Type Oxides for Optimized Lithium-ion Transport. Major Professor: Ernesto E. Marinero.

Current lithium based portable electrochemical storage devices are limited by the inherent instability and volatility of conventional electrolytes materials. Ceramic materials show much promise for use in advanced lithium based battery systems due to their inhibition of dendritic growth and high thermal and chemical stability. The main drawback of solid materials is their low ionic conductivity, relying on lattice hopping to transport ions between electrodes during cycling. Garnet type oxides, specifically of the base compositions $Li_7La_3Zr_2O_{12}$ and $Li_5La_3Bi_2O_{12}$ have been synthesized through Pechini method solution based processing by the dissolution of reagent salts into nitric acid and creation of a chelated polymerized complex. Through an extensive examination of the subsequent processing conditions, it is revealed that the many contributing factors in this process can be optimized to create mixtures of these two structures. By changing the composition, the structure-property relationships between $Li_{7-x}La_3Zr_{2-x}Bi_xO_{12}$ compounds are examined demonstrating that stoichiometric variations offer improvements to both the degree of sintering and the ionic transport in this promising class of materials.

CHAPTER 1. ENERGY STORAGE MATERIALS

1.1 Introduction

There is a significant and growing demand for clean energy for portable applications to meet society's needs and diminish technological contributions towards pollution and global warming. A significant portion of the energy used by society is derived from the transformation of stored chemical energy, specifically in the form of hydrocarbons and fossil fuels, which lead to pollution of the environment through the release of greenhouse gases. Renewable and environmentally friendly energy harvesting technologies including wind and solar are being developed to satisfy the world's growing demand for clean energy with portable applications; yet the power generated from renewable sources comes in fluctuating intensities and necessitates storage to be useful. Furthermore, portable energy sources are required for mass transportation applications. The increasing demand for energy storage has motivated considerable research and development, resulting in light and energy dense chemical storage systems which allow energy to be stored, transported and converted to thermal, electrical and mechanical energy. Ultimately, at the heart of cutting-edge energy storage systems lies the development of novel materials. In the following chapters, a novel method for producing advanced battery materials will be examined in detail.

1.2 Electrochemical energy storage

Electrochemical energy storage systems convert energy stored by chemical bonds into electrical energy as redox reactions occur to form more thermodynamically stable species. The driving force behind these reactions is the Gibbs free energies of formation between products and reactants in a given chemical system. When the reactants and products are able to be physically separated, electrochemical cells can be created wherein redox reactions occur at two separate locations or electrodes. To collect electrical energy from the reaction, the electrodes must be separated by a poor electrically, yet high ionically conductive material for ion transport. An external electrical conduction to the electrodes enables one to utilize the associated electrical current produced. The electrochemical cell functions by completing two redox reactions: an oxidation reaction at the anode, and a complementary reduction reaction at the cathode. A voltage can be measured between these electrodes which is proportional to the driving force of the chemical reaction. To prevent the reaction from completing when the circuit is open, a balancing electrostatic force in the electrolyte prevents the reaction from progressing by inhibiting ionic transport from short circuiting the cell. When the circuit is closed, the reaction proceeds as dictated thermodynamically. After completion of the reaction, when the cell is in a discharged state, an external voltage can be applied to drive the reverse reaction in secondary batteries; this is contrasted to primary batteries, which are single-use systems and as such, not rechargeable.

Batteries based on the alkali metal lithium are of great interest in the development of energy storage systems due to this light and reactive element’s characteristic high theoretical

specific energy. Pioneered in 1979, secondary lithium-ion batteries take advantage of "shuttling" energy between the anode where it resides in the charged state, and the cathode where the lithium dwells in the discharged state of a battery [1]. Conventional secondary lithium-ion batteries employ intercalating electrodes such as graphite (anode) and $LiCoO_2$ (cathode) as shown in Figure 1.1.

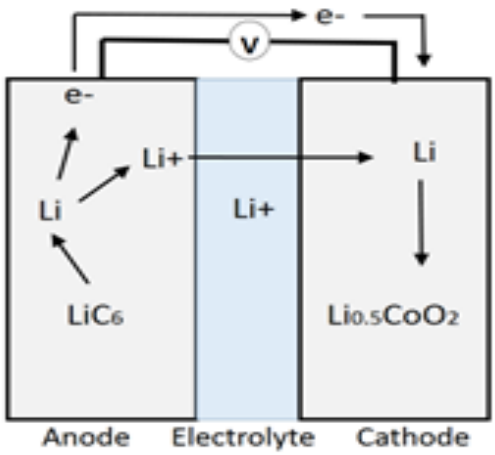

Figure 1. Schematic of a typical lithium-ion battery with graphitic anode and lithium cobalt oxide cathode.

An ideal anode would utilize only pure lithium metal because of the large weight and volume to energy ratio savings this would offer compared to intercalating anode architectures. Lithium-sulfur and lithium-oxygen systems are promising prospects for future energy storage systems due to the replacement of intercalating oxide based cathodes. When altering the base chemistry of the cell (e.g. from lithium-ion to lithium-sulfur), the Gibbs free energy of reaction changes, altering the driving force and changing the reaction kinetics. Although the more progressive technologies such as lithium-air utilize less weight-reliant cathode combinations than lithium-ion batteries, ultimately the battery reaction can still be bottlenecked by slow transport between the electrodes. In the same

way, other chemistries based around metals like sodium, zinc, and aluminum are different from lithium based batteries, but they all likewise require sufficient ion transport between the electrodes.

1.3 Electrolytes

As mentioned, there are three main components of a battery: anode, electrolyte, and cathode. The electrolyte serves a variety of functions in the electrochemical cell as an integral component that interfaces with both of the electrodes. In a secondary battery, a basic electrolyte must allow for rapid transport of charge carrying ions, while remaining electrically insulating, chemically inert, and retaining its properties over many cycles.

Conventional lithium-ion batteries employ lithium salts dissolved into organic solvents as electrolytes because they have a fast ionic transport rate, operate under ambient conditions, and are easy to incorporate into many battery form factors. Having no shape, these liquids require the use of a solid material, the separator, to keep space between the electrodes. When solvated, common lithium salts such as lithium hexaflourophosphate ($LiPF_6$) dissociate into the respective anions (PF_6^-) and cations (Li^+), allowing for independent motion within the fluid. The room temperature ionic conductivity of these liquid electrolytes is on the order of 10^{-2} S/cm [2]. However, the total ionic conductivity of a liquid electrolyte is not the same as the ionic conductivity of the lithium-ions in solution; anions also are able to carry the charge, implying that the total transference from cation mobility (t^+) is only a fraction of the whole and related to the cationic and ionic currents (i^+ and i^-) respectively):

$$t^+ = \frac{i^+}{i_{total}} = \frac{i^+}{i^- + i^+} \qquad \textbf{Eq. 1}$$

It is therefore desirable to have lithium salts with large anions with slower relative mobility. Ionic mobility and transport also scales inversely with viscosity in that a more viscous system will have a lower ionic conductivity [3]. Mixtures of organic solvents are often used to create liquid electrolytes because no single solvent possesses all the properties optimizing lithium-ion transport [3], [4].

Although they provide many ideal properties, mixtures of organic solvents and salts common to lithium-ion batteries leave much to be desired as electrolytes. Interfacing with the electrodes for optimal lithium transfer is an important electrolyte function, and not all electrolyte-electrode pairs function properly. Due to the high activity of the anode, a "solid-electrolyte interphase" (SEI) is typically formed at the boundary between electrolyte and electrode [5]. Though often engineered to maximize cell life, the SEI can serve as a nucleation point for dendritic growth, a common failure mechanism for secondary batteries [6]. Solutions such as advanced separators are being explored which mitigate the dendritic problems, but do not completely eliminate the issue. Furthermore, other issues with organic electrolytes such as toxicity, flammability and other safety related concerns may not be completely solved by advances with separators. Safer and less toxic ionic liquids can also be used, but suffer from the same compatibility issues with reactive electrode materials. In summary, liquid electrolytes have many advantages, but pose many problems when included in current ion-shuttling batteries. Solutions to these problems will require a critical

look at the underlying mechanisms of electrolyte functionality and exploration of different materials and production for incorporation into future battery systems.

1.4 Alternative electrolyte systems

Thus far, liquid electrolyte systems have been briefly explored. Overall, mass transfer is much more rapid through these liquids when compared to solids of equal dimensions. General material tradeoffs between the different classes of materials indicate that solids will have a decreased ionic conductivity, but often are able to make up for the lack of stability and safety presented by disordered liquid systems. Materials for solid electrolytes bring increased functionality to the cell in terms of stability, safety, and even cyclability. If the mechanisms of lithium-ion conduction in these materials can be optimized, battery safety, lifetime, and capacity can be improved significantly.

1.4.1 Polymer based ion conductors

Polymers have been explored as an alternative to liquid electrolytes due to their functionality as a solid material, allowing safer operation, cell compaction (decreased distance between electrodes) and mechanical integrity. Early studies with polymer electrolytes found that they can conduct ions significantly better when they are amorphous, or above their glass transition temperature (T_g) [7], but they still possess relatively poor ionic conductivities at ambient temperatures on the order of 10^{-8} - 10^{-4} S/cm, orders of magnitude less than that of liquid electrolytes. This is even the case when they are mixed with lithium salts in a similar fashion to that of their organic liquid alternatives [8]. These “dry” polymer electrolytes have a high molecular weight, which change properties slightly when they dissolve the lithium salts required for ionic conduction. [2]. Dry polymers can

be modeled to conduct lithium ions as expressed by the Vogel-Tammann-Fulcher equation [9]-[12]:

$$\boldsymbol{\sigma = A T^{1/2} \exp\left[\frac{-B}{(T - T_g)}\right]} \qquad \textbf{Eq. 2}$$

In this equation, *A* and *B* are constants for a given materials system. As can be readily seen by this equation, polymer ionic conductivity will increase with temperature, as the system approaches its T_g. Interestingly enough, the T_g is lowered by adding more lithium salts and increasing the disorder of the system [7]. Instead of relying solely on ionic motion through an amorphous network, polymer electrolytes can be enhanced by the addition of traditional organic aprotic solvents [13]. This addition serves to dramatically increase the ionic conductivity, forming "gel" electrolytes in which the polymer forms a backbone for the battery and the organic electrolyte fills in the pores. This is not dissimilar from typical separator architectures, except that the separator may be an active component in this case. Even though there is rapid lithium-ion transport in these systems, they still encounter many of the challenges associated with pure organic liquids in that they can degrade the electrodes and may not be completely safe and stable over a wide range of temperatures and voltages.

Gel polymer electrolytes were introduced in order to mitigate safety and stability challenges associated with conventional liquid electrolytes. Polymer based materials serve to improve upon the unfavorable features of high energy battery systems, but still leave room for improvement; polymers may not be hard enough to completely inhibit dendritic

growth, and are not the most stable. They also fail to conduct lithium at an appreciable high rate. Therefore, other promising alternatives have also been the subject of much investigation.

1.4.2 Ceramic based ion conductors

Attention has been given to the ionic conducting ceramics due to their higher degree of stability in conjunction with a variety of electrode materials and relative stability. Additionally, many of the materials discussed in the following sections are ionic solids, meaning their transference number will be effectively 1 due to the low anionic mobility relative to that of the cationic counter-ions (Eq. 1). Yet as previously expressed, these materials will generally have less favorable ionic mobility, specifically regarding the mobility of interesting components such as lithium cations. Efforts to increase lithium-ion mobility in ceramics often relies upon changing composition and processing methods to modify the defect concentration, microstructure, and lattice parameter of these solid-state electrolytes. By tailoring the properties of ceramics, materials tradeoffs may be overcome to create advanced solid-state electrolytes and improved battery systems offering high ionic conductivity coupled with safety and stability.

In most ceramics, whether amorphous or crystalline, a model for ionic hopping similar to random walk through defects can be used to approximate the ionic conductivity. Such models take into account the vibrational frequency (ω_0), carrier concentration (c), geometric sites for ions (N), jump distance (a), and a correlation factor (γ) to calculate the ionic conductivity in solids [14].

$$\sigma T = Ne^2a^2\gamma c(1-c)k_B{}^{-1}\omega_0 \exp\left[\frac{S}{k_B}\right]\exp\left[\frac{-E_A}{k_BT}\right] = A\exp\left[\frac{-E_A}{k_BT}\right] \quad \textbf{Eq. 3a}$$

$$\sigma = A/T\exp\left[\frac{-E_A}{k_BT}\right] \quad \textbf{Eq. 3b}$$

Equation 3b is often used in a simplified form to report data on ionic conductivity and calculate the activation energy (E_A) required to move a single ion based on the Arrhenius relationship. Additionally, equations 2 and 3b are useful for comparing the temperature dependences of different materials as reflected in Figure 2. This comparison becomes important for selecting the correct electrolyte material for a given battery system and its intended application.

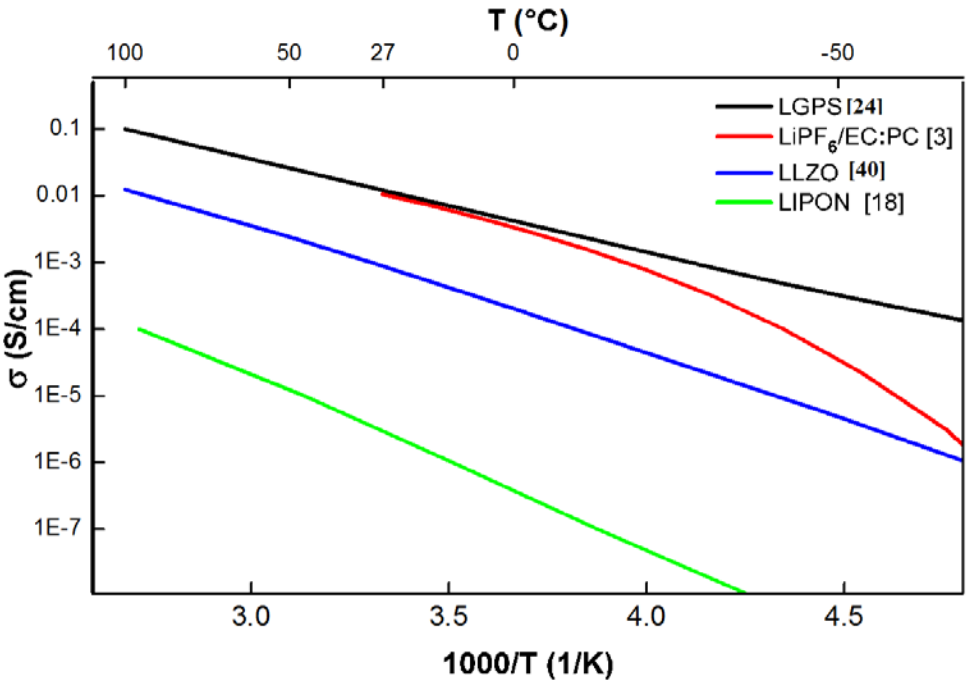

Figure 2. Graph comparing the most promising lithium conducting electrolyte materials and their relative ionic conductivities as a function of temperature. The ceramic materials can be modeled using Arrhenius relationships (Eq. 3b). Adapted from [3], [18], [24], and [40].

1.4.2.1 Amorphous ion conductors

Amorphous solid materials, whether sulfide or oxide based have been of interest since the 1980's due to their easy processing compared to their crystalline counterparts. Specifically, amorphous sulfide compounds have attracted interest over the years due to their high ionic conductivity that dates back to 1981, in which Mercier et. al created Li_2S-P_2S_5-LiI systems that had a lithium-ion conductivity 10^{-3} S/cm at room temperature [15]. Efforts to increase the ionic conductivity of these materials include changing compositional ratios to increase T_g[16]. The sulfide systems are significant more appealing than the oxide-silicate mixtures, such as Li_2O-SiO_2-Al_2O_3, which only has an ionic conductivity values of 10^{-6} S/cm at room temperature [17]. This can be attributed to decreased bond length in oxygen containing materials.

The most commercially available solid-state electrolyte is a nitrogen substituted amorphous version of Li_3PO_4 termed LiPON [18]. The ionic conductivity for this material is only on the order of 10^{-6} S/cm at 25˚C. It is typically created by RF sputtering in a N_2 atmosphere and is stable against lithium metal [19]. Because electrolyte thin films allow for decreased ohmic resistance in batteries; cell functionality is possible with lower ionic conductivities in thin film electrolytes. Thus, the poor ionic conductivity of LiPON is not an issue because it can be created in such thin layers. The versatility of sputtering coupled with an electrolyte with adequate ionic conductivity and high stability are what has made LiPON the most successful solid-state electrolyte to date. LiPON is used instead of the more attractive amorphous sulfides because of their hygroscopic nature.

1.4.2.2 Crystalline ion conductors

A number of promising ceramic electrolytes are crystalline in nature, and as such have a variance in ionic conductivity as a function of lattice parameter and defect density. The rapid lithium-ion transport that occurs through the bulk of the crystalline regions can be orders of magnitude faster than what occurs in the grain boundaries [20]. The best crystalline ceramics are summarized here.

One of the first crystalline ceramics to be intensely scrutinized was named **LI**thium **S**uper **I**onic **CON**ductor (or LISICON) because of its high ionic conductivity [21], [22]. Original LISICON had the structure of $Li_{14}Zn(GeO_4)_4$, where aliovalent dopants such as zinc have been substituted into the structure. This substitution stretches the lattice, increasing the bond distance between the GeO_4 tetrahedrons and the lithium channels, thus increasing the ionic conductivity. Although the LISICON structure boasts ionic conductivity on the order of 10^{-1} S/cm at 300 ˚C, it drops off several orders of magnitude to 10^{-7} S/cm at 30 ˚C. However, substantial improvements to the chemical properties have been made with the substitution of sulfur anions for the conventional oxygen, greatly stretching the lattice as pioneered by Kanno in 1999, forming thio-LISICON [23]. This structure has been modified to create $Li_{10}GeP_2S_{12}$ shown in Figure 2, which conducts Li-ions at 25˚ on the order of 10^{-2} S/cm, which is comparable to most organic liquid electrolytes [24]. The primary drawback of this material is that hygroscopic sulfide composition, requiring specialized fabrication environments. The evolution of LISICON to thio-LISICON structure shows how dependent the transport properties of a material can be on the surrounding structure.

Crystalline ceramics that have also been examined in great detail are the NASICON, and perovskite systems. Similar to LISICON, is the NASICON-type ceramics have the name Sodium (**Na**) **S**uper **I**onic **CON**ductor and a crystal structure with the stoichiometry $NaM_2(PO_4)_3$ (M=Ge, Ti, Zr). In this structure, each of two M-sites can be individually composed of different elements [25], [26]. This leads to many different compositions as constituent elements can reside on multiple places within the lattice [27]. In the same way with LISICON and NASICON, the Perovskite type ceramics with a composition of $Li_{3x}La_{2/3-x}TiO_3$ (LLT) have also shown high ionic conductivity of 10^{-3} S/cm at room temperature, which can be modified with lattice stretching and ensuing opening up of lithium migration pathways [28], [29]. These materials have high ionic conductivity from a large amount of lithium site vacancies introduced into the system just by changing the amount of lithium used in the formulation [30]. Ultimately, almost all ceramic materials behave similarly and obey the same rules. It is also the case that for these systems that they suffer from poor grain boundary conduction of lithium ions when compared to the bulk of the samples [31] – [33]. Therefore, much effort has been focused on increasing the densification of these promising materials, which require high temperatures in excess of 1100 ˚C to obtain the desirable properties. Still, the high sintering temperatures used to create the coarsened structures can result in lithium loss, making the composition difficult to control. Much current research is focused on densification and mitigating grain boundary resistance to lithium transport in these materials.

1.5 Crystalline garnet type oxides

A comparable and recently discovered crystalline class of ionic conductors, garnet-structured oxides, are stable against Li metal and have ionic conductivities on the order of 10^{-4} S/cm [34]. Although not possessing quite as high of ionic conductivity as some of the other ceramics, garnets of the chemical formula of $Li_5La_3Ta_2O_{12}$ have shown the same increases with lattice stretching by substitution of the lanthanum and tantalum sites [35], [36]. Garnets also suffer from poor densification similar to that of NASICON and perovskite structured electrolytes. However, aluminum has been introduced to help stabilize the cubic phase and densify grain boundaries [37], [38]. To date, zirconium-doped garnet type oxides of the formula $Li_{5+x}La_3Ta_{2-x}Zr_xO_{12}$ demonstrate comparable ionic conductivity to that of the other ceramic materials on the order of 10^{-3} S/cm at room temperature [39]. A major advantage of this class of materials is that they are able to maintain contact with pure lithium metal, and are relatively stable at ambient conditions, which is not the case of many of the other types of crystalline ceramics. Garnets type oxides represent a promising group of materials that has come to embody the effects of aliovalent doping to increase ionic conductivity and exhibit many desirable qualities for use as an electrolyte material.

1.5.1 Processing of Garnet type oxides

As previously discussed, many electrolyte materials are capable of high ionic conductivity at room temperature, as shown in Figure 2. Therefore, electrolyte material selection should focus on other materials properties (e.g. stability, volatility) and ease of fabrication. Oxides are generally stable and able to be produced under ambient conditions, whereas sulfur

based materials are typically volatile and must be created and handled in oxygen and water free environments. Of the oxide materials, garnets are the most promising due to their high chemical stability and ability to interface directly with lithium metal and over a large range of voltages [40]. Under these conditions, titanium containing lattices of the NASICON and perovskite type materials will become increasingly electrically conductive [31]. As such, the remainder of this document will focus on garnet type oxides and ways to produce them.

Ceramics, as a more promising class of electrolyte materials for certain lithium based batteries, are significantly more difficult to insert between electrodes when compared to liquid/separator combinations or polymers. Soft materials can be easily inserted or fit to existing electrodes. On the other hand, ceramic materials typically require heat treatment to create a desirable microstructure, chemically bond to the electrodes, or both. Theory aside, important considerations must be made towards implementation of electrolytes into functional battery systems. Thus, processing becomes an important consideration for materials selection in fast Li-transporting materials. LiPON, a material with moderate Li-ion conductivity, has a definitive and reproducible method of easy and scalable fabrication making it ubiquitous in a Li based energy storage. Processing is a significant factor that must go into consideration for materials selection when discussing technologies such as batteries.

The complex oxide materials discussed previously all require significant amounts of time and heat to create crystalline domains and mitigate grain boundary resistance to ionic transport. To decrease the energy required for crystal growth, dopants can also act as sintering aids, densifying samples at reduced temperature or decreasing the activation

energy for phase formation [37]. Conversely, processing methods can be altered to lower synthesis temperature. Conventional solid-state fabrication relies on inefficient mechanical milling and sintering; alternatives methods such as sol-gel or polymerized-complex can reduce the temperature required for electrolyte fabrication [41] – [43]. Calcination of these solution-based complexes produces more homogeneous powder mixtures, freeing the process from time consuming mechanical mixing. Additional work is required to further decrease formation energy of crystalline regimes in lithium-ion conductors, whether through doping or processing.

1.5.2 Compositional variations of the garnet type stoichiometry

Garnet oxides of the crystal structure $A_3B_2(CO_4)_3$ family have been demonstrated as reliable structures upon which to create electrolytes through aliovalent doping, the doping of different elements with other valence states into an existing structure [44]. In the "lithium stuffed" garnets discovered by Thangadurai et. al, lanthanum sits on the A sites with 8-fold oxygen coordination, tantalum sits on the B site with 6-fold coordination, and lithium sits on the C sites with 4-fold coordination; additional lithium sites are also added to the lattice, decreasing the lithium jump distance and increasing the ionic conductivity [34]. The lithium sites (up to 5 formula units from 3) are added to maintain charge neutrality in the lattice and settle on interstitials sites to form complex lithium migration pathways [45]-[47]. The amount of lithium in the lattice was further increased to 6 formula units through substitution of calcium, strontium, and barium onto the B sites in the lattice for lanthanum [35], [48] and further to 7 with the introduction of zirconium onto the A sites [49]. Due to its lower valance (Zr^{4+} vs. Ta^{5+}), the zirconium ions substituted into the

structure and introduced new lithium interstitial sites in this cubic lattice [50], significantly enhancing the ionic conductivity. To date, $Li_7La_3Zr_2O_{12}$ (LLZO) and similar zirconium-doped garnet type oxides have recorded the highest ionic conductivity values. The additional lithium sites in the lattice allow for degeneracy of lithium migration pathways, and thus increase the correlated motion of lithium through the structure under an applied potential.

The first challenge of LLZO based garnets was inhibition of the tetragonal phase formation, a phase which conducted lithium-ions two orders of magnitude worse than the cubic garnet phase. The more ordered tetragonal phase is formed when lithium-ions settle into ordered positions farther apart in the lattice [51]. In order to preferentially create cubic garnets, zirconium sites are partially substituted (typically <50% occupancy) by ions of higher valances [39], [52]-[54]. This serves to not only stabilize the cubic phase, but also optimize the ratio of lithium-ions to lithium-vacancies in the lattice and maximize ionic conductivity.

The other significant challenge to LLZO electrolytes deals with incomplete densification during low temperature fabrication. It was discovered that aluminum contamination through the use of alumina crucibles acted to stabilize the cubic phase of LLZO and improve ionic conductivity [49]. With further investigation, it was suggested that aluminum acts simultaneously as a sintering aid and dopant onto lithium garnet sites in the cubic lattice, stabilizing the cubic LLZO and lowering fabrication temperature [37]. In light of these studies, similar dopants such as gallium and germanium have also been used to substitute onto lithium occupied C sites in the lattice [55], [56]. Due to their positions on the lithium sub-lattice, these dopants may slightly decrease the rate of lithium migration

through lithium channels [57]. However, it is a contested point in the literature if this is in fact a factor that affects the ionic mobility [58]. In short, alternative doping schemes may result in increased ionic conductivity and improved processability of garnet type oxides.

The fabrication process plays also a key role in determining the properties of solid state ion conductors. Conventional ball milling and sintering techniques without dopants can require as much as 36 hours at 1230 ^{0}C for stabilization of the cubic phase and subsequent densification is necessary to achieve ionic conductivities on the order of 10^{-4} - 10^{-3} S/cm [34]. Fortunately, sol-gel and polymerized complex fabrication techniques such as the Pechini method have been utilized to create a more homogeneous mixture of precursor material, reducing the activation barrier for complete mixing [38], [42], [61]. By simultaneously employing doping, or combinatorial mixing of existing garnet oxide materials and solution based fabrication, improvements can be made in terms of both materials properties such as ionic conductivity, as well as densification. In other words, judicious dopant selection and site-specific substitution, can be employed to tailor the garnet composition for optimized ionic conductivity at lower temperatures.

CHAPTER 2. SOLUTION BASED PREPARPATION OF GARNET TYPE OXIDES

2.1 Materials and methods for production

Pechini method synthesis was used to fabricate the complex garnet type oxides with cations of lithium, lanthanum, zirconium, and bismuth. To help promote consistency with the synthesis and avoid potential contaminations, all the metal salts used were nitrates even though other salts such as chlorides may achieve the same results. The main requirement for these experiments is that the salts are soluble aqueous solutions. Salts used were $LiNO_3$, $La(NO_3)_3 * 6H_2O$, $ZrO(NO_3)_2 *xH_2O$, and $Bi(NO_3)_3 * 5H_2O$. In order to determine the amount of hydration for the zirconium salt, thermogravimetric analysis was used on a pulverized amount of the reagent chemical. From the final mass, the number of water molecules can be stoichiometrically calculated.

The first task with in the synthesis is to get the salts into solution. It was found that the lithium and lanthanum salts readily dissolved, but the zirconium salt dissolved slowly and the bismuth salt would not completely dissolve in heated water even after 24 hours. The bismuth nitrate would, however, dissolve in diluted (5-15%) nitric acid when heated. As such, it was useful to dissolve the bismuth salt first into hot nitric acid, wait until completely dissolved, and then continue adding the other reagents. It was observed that if the zirconium was added before the bismuth was completely dissolved, the solution could remain a colloid with the bismuth not dissolving completely.

After complete solvation of all the salts, other components were added to promote the synthesis of the polymerized complex. The ultimate goal of this synthesis was to create a homogeneous distribution of metal ions and surrounding polymerized matrix. Citric acid was used as a chelating agent and ethylene glycol was also added as a complexing agent. The purpose of adding the chelating agent was to bond to the cations in solution; it was also observed that at times the chelating agent may have helped with solvation of the ions. It was assumed that all the bonding was uniform between the cations and the chelating agents in that no metal ion was preferentially chelated because the citric acid was not typically added until all the ions had been dissolved into the solution. In the hot, acidic conditions the aqueous solution was subjected to, the addition of the ethylene glycol would allow for polyesterfication, or polymerization between the ethylene glycol and citric acid molecules. Thus, the citric acid and ethylene glycol were ideal additions to the nitric acid, cation containing solution to create a homogeneous polymerized complex for subsequent heat treatment and creation of a complex oxide powder to be used as an electrolyte.

A couple of ratios were important for changing the processing of the polymerized complex. The first ratio is that of ethylene glycol to citric acid, which was important for preventing auto-ignition of the resultant polymer during heat treatment. If the ratio was too high or too low, auto-ignition was observed upon calcination similar to that reported by Reichenbach and McGinn [59]. The primary ratio used was 40: 60 of citric acid: ethylene glycol. This ratio was useful because it was the limit about which auto-ignition would not be observed, while having sufficient ethylene glycol to allow for polymerization between the citric acid molecules. The second ratio of importance was that of total organic to metal cation. The

ratio typically used was 62: 38 of organic: metal. This ratio kept the citric acid to total metal ratio close to one allowing for near unity chelation. Furthermore, it provided enough organic to chelate and polymerize in solution relative to the total number of cations. It would be possible to use a larger proportion of organics, but that could lead to waste of reagents and lower yields for each calcination heat treatment due to size limitations on the furnaces. An increase in these ratios may be necessary to complete the reaction under some conditions.

Finally, upon dissolution of all the constituent reagents, the reaction is left to sit on a hot plate at 80 °C for up to 48 hours, during which it reacts. With sufficient time and temperature for reaction to occur, the residual solvent is allowed to evaporate and the polymerized complex is heated at 200 °C for 12 hours to harden the polymerized complex into a brown plasticized mass, which can be heat treated. In early experiments, the solution was just left to sit in an open beaker, and aliquots of dilute nitric acid were periodically added to keep the polyesterfication reaction progressing for up to 48 hours. However, reproducibility proved difficult as nitric acid (T_b = 83 °C) evaporated rapidly from the solution and could halt the reaction. To allow for a more streamlined process, a refluxer and round bottom flask were used instead. These led to a slight difficulty in controlling temperature homogeneity for the given process, which will be discussed in section 2.3.

2.2 Heat treatment to produce complex oxides

A minimum of a two-step heat treatment is necessary in order to process the homogeneous polymerized complex to create a useful solid state electrolyte material. The first step in this process is the calcination of the polymerized mass. Calcination is a thermal treatment whereby the polymer is decomposed at high temperatures and a chemical

reaction takes place. In this case, at high temperatures, various forms of carbon, aldehydes and other organic derivatives are formed as the polymerized mass decomposes; the heavy metal cations, which are not as easily transformed into the gas state are subsequently oxidized – typically with oxygen. If little or no metal cations were vaporized in this part of the heat treatment, the resultant stoichiometric ratios of the cations in the oxide formed should be the same as that of the solidified precursors. The second step in the heat treatment is the sintering process. Here, a pellet is pressed from the calcined motherpowders. This green body is then heat treated to allow for densification of the powders. In this second step of the process, no major chemical reactions should take place. Small scale reactions may take place, such as the local ordering of individual ions within the grain boundaries, or vaporization of a certain small elements. Nevertheless, these reactions in the sintering process are not on the same level as the major chemical changes that occur during the calcination process.

2.2.1 Calcination of polymerized complexes

Calcination of the polymerized complex was an important and complicated step in the process. Compositional differences in the cation stoichiometry could affect the necessary calcination temperature to form the phases necessary as described in section 1.5. It is necessary to input enough heat to not only decompose the polymer matrix, but also allow for sufficient activation for the complex oxide to self-assemble into the desired structure. The first step in this process is to perform thermogravimetric analysis (TGA) of the polymerized complex. TGA curves show at which temperature a given sample loses mass when heated as components of it are vaporized. Figure 3 shows the TGA curve for a typical

precursor powder which has been completely synthesized. The large drop around 300 ºC is the mass loss due to the decomposition of the polymerized complex. Other small mass losses are seen between 500 ºC and 600 ºC. These artifacts can be ascribed to the carbon in the organic derivatives forming carbonate species with some of the metal ions as they oxidize. However, it is outside the scope of this work to examine the specific kinetics of what is going on in this case. The main conclusion that can be drawn from this curve is that a minimum temperature of approximately 600 ºC is required to get rid of a majority of the organic impurities and leave behind oxide materials. Calcination below this temperature may lead to impurities from carbon being incorporated into the samples.

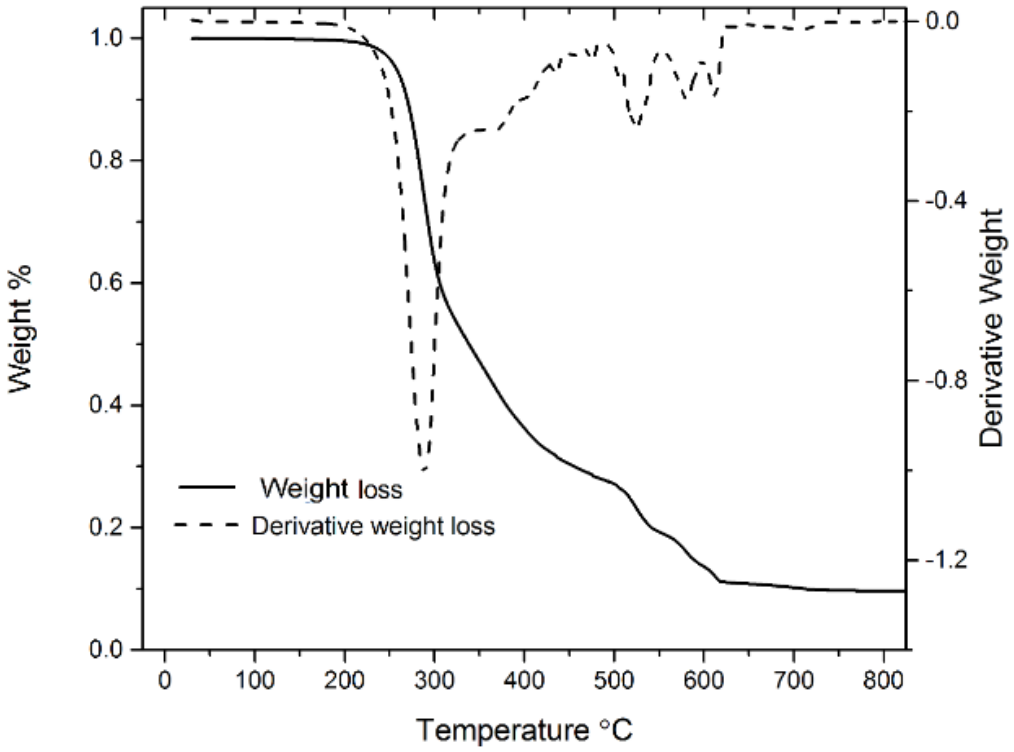

Figure 3. Thermogravimetric analysis of a completely reacted polymerized complex.

When the minimum temperature for calcination is known, the next logical step is to determine the energy required for desired phase formation for the respective systems of interest. Figures 4 and 5 examine the phase formation through X-ray diffraction for different temperature heat treatments of garnet type oxides $Li_7La_3Zr_2O_{12}$ and $Li_5La_3Bi_2O_{12}$.

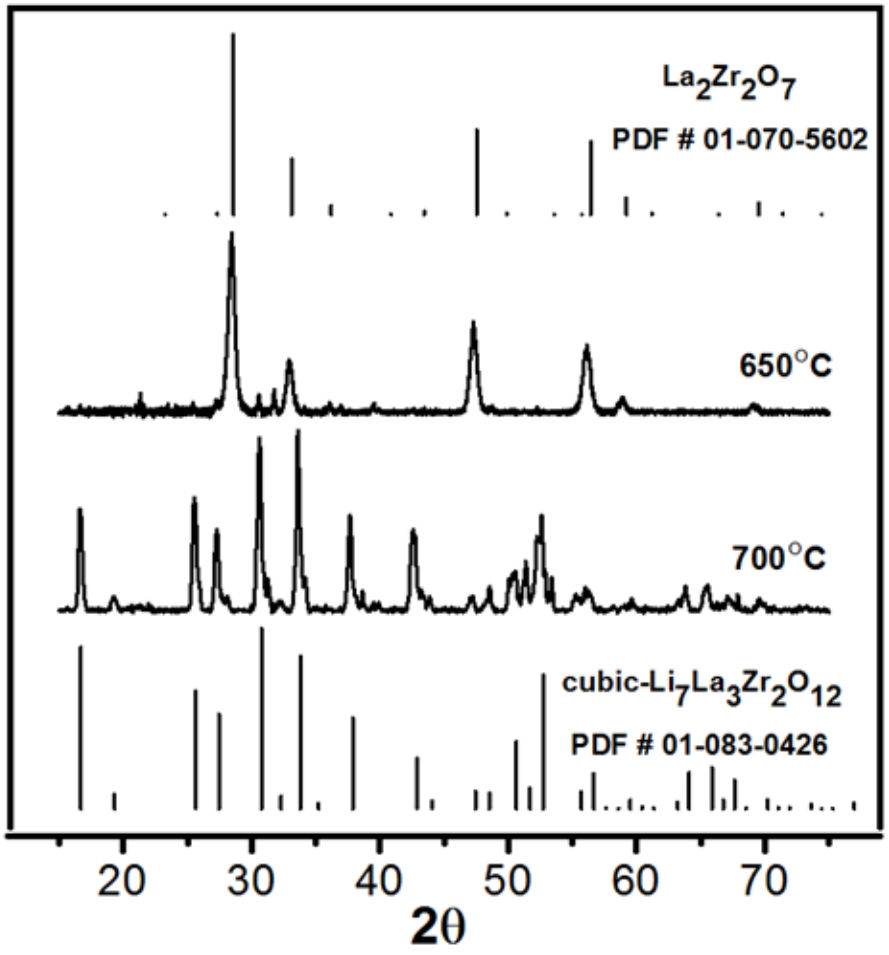

Figure 4. X-ray diffraction intensity - 2Θ patterns for 650 ºC and 700 ºC calcination temperatures of polymerized complexes for garnet type oxide $Li_7La_3Zr_2O_{12}$.

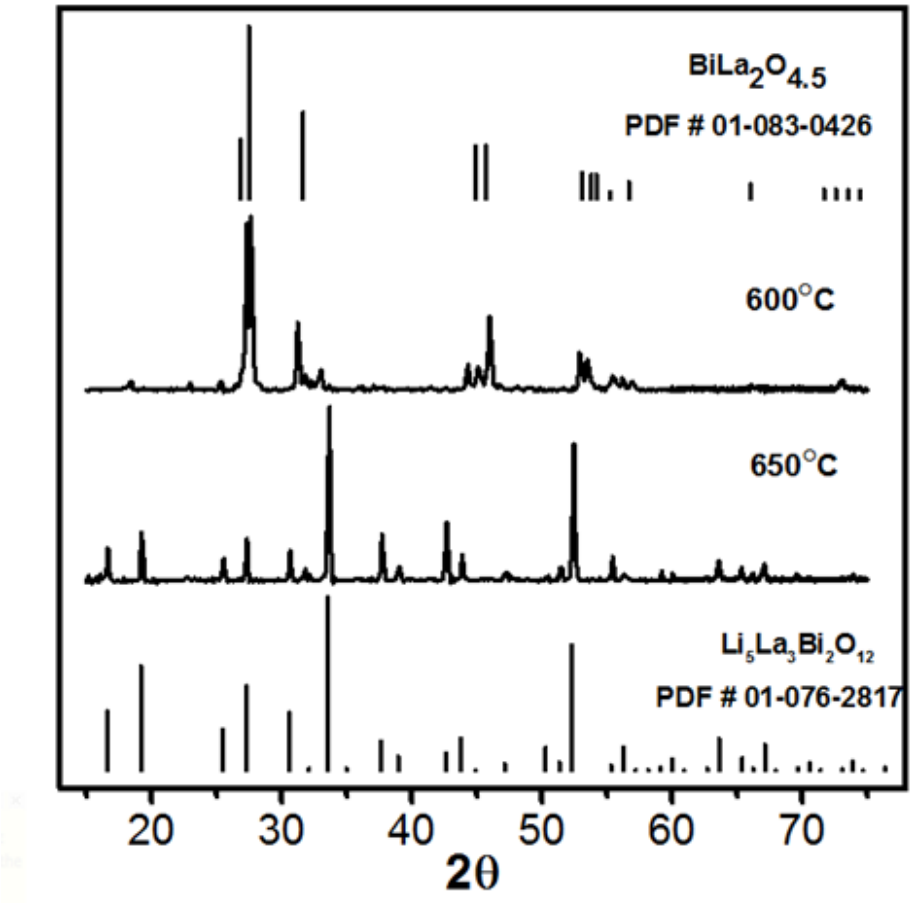

Figure 5. X-ray diffraction intensity - 2Θ patterns for 600 ºC and 650 ºC calcination temperatures of polymerized complex for garnet type oxide $Li_5La_3Bi_2O_{12}$.

Several observations can be made from figures 4 and 5, both individually, and when compared to one another. The first observation is that the cubic garnet type phases are both formed above 700 ºC. However, for the sample containing only zirconium, the temperature is higher because the phase transition from precursor $La_2Zr_2O_7$ pyrochore-type phase of space group Fd-3mZ into an Ia-3d garnet cubic phase does not take place until 700 ºC. Whereas the bismuth sample undergoes the same transition from a similar phase transitions from space group R-3mH $BiLa_2O_{4.5}$ at 650 ºC. Although the precursor space groups are

not the same, they have a lot of comparable symmetries and eventually transition into the same cubic garnet-type structure.

2.2.2 Sintering of precursor motherpowders

Following calcination and formation of the complex oxide powders as confirmed by x-ray diffraction, the powders can undergo additional heat treatment to make them testable for other properties such as density and ionic mobility. To get them into a circular pellet that can be tested, they were first ground with agate mortar and pestle for several minutes before uniaxial pressing into 12mm circular die at 40MPa for 10 minutes. The pressed pellets, or green bodies, were submerged in the ground up precursor mother powder to avoid lithium and bismuth volatilization at high temperatures. These submerged green bodies were then heat treated at temperatures higher than 800 °C in a magnesia crucible to prevent contamination from the high temperature process. Typical heat treatment was at 900 °C for 10 hours with a ramp rate of 5 °C/min. Higher heat treatments were tried on $Li_7La_3Zr_2O_{12}$ and $Li_5La_3Bi_2O_{12}$ pellets to observe the effects of higher temperatures on alternate phase formation. Although, as expected, $Li_5La_3Bi_2O_{12}$ remained cubic up until over 1000 °C at which point it decomposed, whereas $Li_7La_3Zr_2O_{12}$ undergoes a phase transition around 950 °C from a cubic symmetry to tetragonal as shown in Figure 6.

Figure 6 illustrates the tetragonal phased garnet type oxide of composition $Li_7La_3Zr_2O_{12}$ which was calcined at 700 °C for 10 hours and then pressed and sintered at 900 °C and 950 °C respectively for 10 hours. Structurally, this phase transition from the cubic symmetry to the tetragonal is just that of one direction in the repeating unit cell lattice structure

compressing, given that in tetragonal structures a = b ≠ c, whereas cubic structures have all unit cell dimensions the same. This change is observed in the literature, and has been attributed to sufficient activation towards the more stable and ordered garnet-type tetragonal phase [61]. It is possible that this tetragonal phase was more stable at the lower calcination temperatures, but there was insufficient thermal activation to allow for the lattice to get properly ordered.

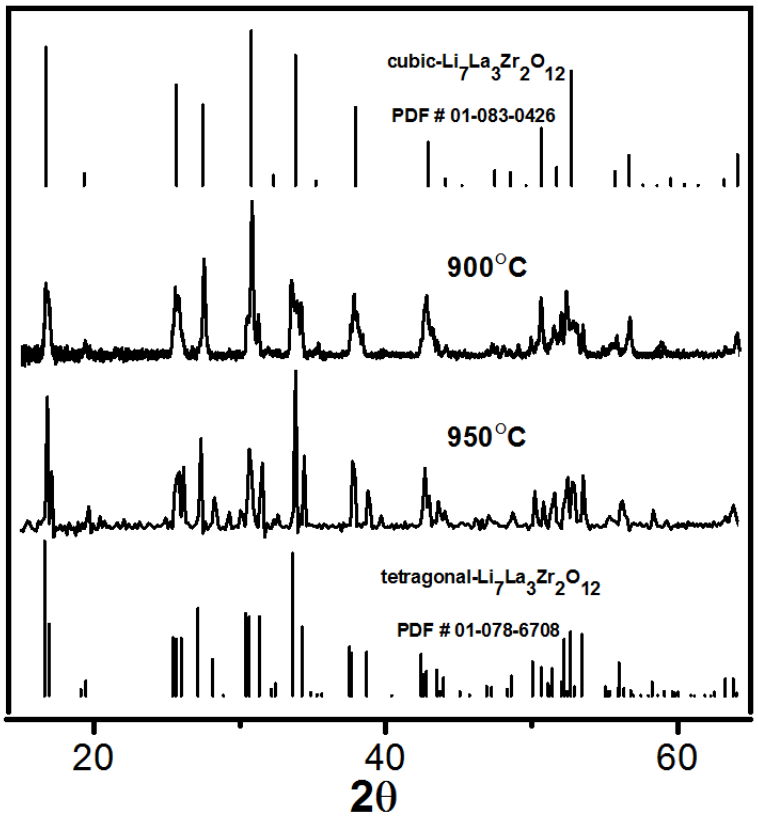

Figure 6. X-ray diffraction intensity - 2Θ patterns for pressed pellets of $Li_7La_3Zr_2O_{12}$ sintered at 900 °C and 950 °C for 10 hours.

No significant chemical changes were expected during this process, nor were any typically observed. The main observations from the sintering trials was the shrinkage of the pellets,

specifically the bismuth containing pellets, and potential volatilization of lithium, which was observed with color change in pellets not covered in the motherpowder. Notably, in cases where an alumina or zirconia crucible was used, some pellets would react with the crucibles as was apparent from significantly crucible warping or cracking, which is unexpected at moderate heating rates less than 5 °C/min. Only moderate discoloration occurred with the use of magnesia crucibles.

2.3 Variability of processing parameters

It was oftentimes the case that the kinetics of the solution based Pechini method reaction yielded perplexing results. The following section will help to shed some light on things that can go amiss during the synthesis and ways to diagnose the problem if unexpected phases occur during heat treatment. The primary factors that have been shown to have great effect on the end stoichiometry and phase of the resultant complex oxide powder are reaction temperature and reaction time. Yet, even with careful control of the process, something may still be wrong with the final product. Possible reasons for this are also discussed below.

As there can be many different polymer structure needed to create the polymerized complex and eventually complex oxide material, a close control of polymerization is not completely necessary for the purposes of this synthesis; even if they may help. It is also of interest to create as much ceramic powder as rapidly as possible to perform additional characterizations and experiments. Therefore, it would be advantageous to speed up the polymerization process. There are many factors governing how fast the polyesterfication reaction occurs, but the important main variables are concentration of the acid,

concentration of the reagents, and heat applied. With a greater concentration of the acid and reagents as well as with an increased application of heat, the reaction can proceed faster and one would have a more desirable higher produce production rate. However, there are some limitations to how high of temperature and how concentrated one can go. The primary limitation ends up being how soluble the metal cations will remain under certain conditions the solution is subjected to. With too low of temperature, the reaction does not proceed at all. Yet, with too high of temperature, the reaction also does not proceed because all the nitric acid is volatized or breaks down into nitric oxide gas – that is, the acid concentration approaches 0. Furthermore, when the acid concentration drops due to high temperature, solid white precipitates begin to crash out of the solution.

Figure 7 shows the XRD patterns of the powders these precipitants create when calcined at 750 °C for 10 hours. The initial sample stoichiometry of this batch was $Li_6La_3ZrBiO_{12}$ and the solution mixture was reacted at 100 °C for several hours before it began to form precipitates. It can be inferred from the diffraction patterns that the precipitants are primarily the larger ions of either zirconium or bismuth as they are not able to form any garnet-type phases with what should be sufficient heat treatment. Additionally, the bismuth nitrate salt was insoluble in regular water, so if the pH drops, it is logical that it becomes insoluble in this solution, even if it is chelated to the citric acid. What is especially interesting is that this implies that there may be a non-uniform chelation of the metallic ions in the solution. For example: the lithium ions may be more strongly chelated and less likely to crash out of solution if there are variabilities in the synthesis. This may lead to

possible inhomogeneous distributions of cations in the polymerized complex and eventually in the final complex oxide powder.

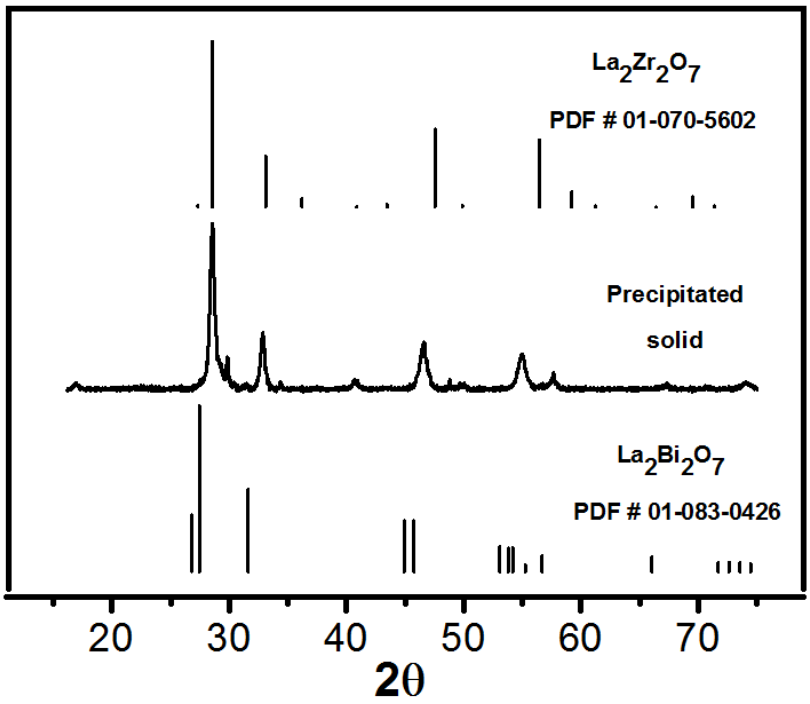

Figure 7. X-ray diffraction intensity - 2Θ pattern for the precipitated solid calcined at 750 °C for 10 hours.

As expected, the previous polymerized complex was not completely reacted which can be seen by the TGA shown in Figure 8. Instead of having a singular large mass loss near 300 °C, there are several mass losses likely due to the piecewise decomposition of the organic additives as they have not fully reacted. Figure 7 also shows mass loss at higher temperatures indicating that residual impurities from the synthesis do not leave readily if the reaction is not fully complete.

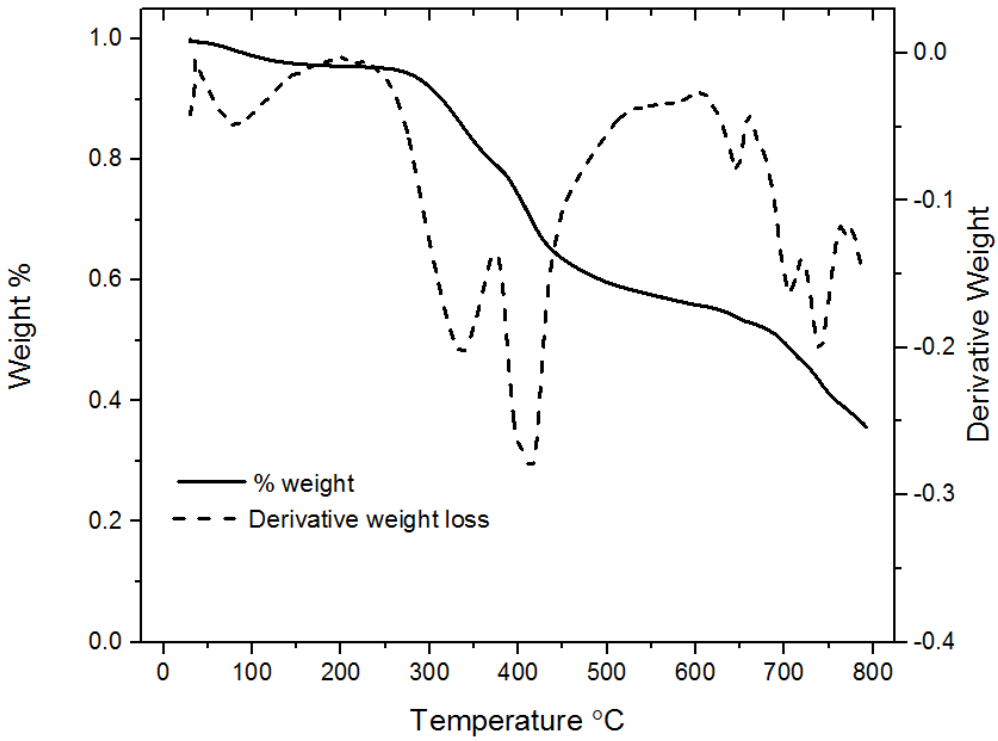

Figure 8. Thermogravimetric analysis of an incompletely reacted polymerized complex.

Finally, although all things may go correctly in the synthesis, there is still a possibility of undesirable phases forming. Figure 9 shows two samples from the same batch that were both calcined at 750 °C for 10 hours, but ended up with different phases forming. The phases present are $La_2Zr_2O_7$ (# peaks) and La_2O_3 (* peaks). Were these samples from different batches, this would be an issue of non-stoichiometry, or different sample compositions. Even though they are from the same batch, this may still be the case here. During the final evaporation of the solvent post reaction, the acidic portion of the solvent may evaporate first, leaving the larger ions crash out and create macro level heterogeneous areas in resulting polymerized complex. Therefore, with all experiments, it is important to

physically grind and mix the resulting polymerized complexes well before beginning any calcination, even if the synthesis is fully completed.

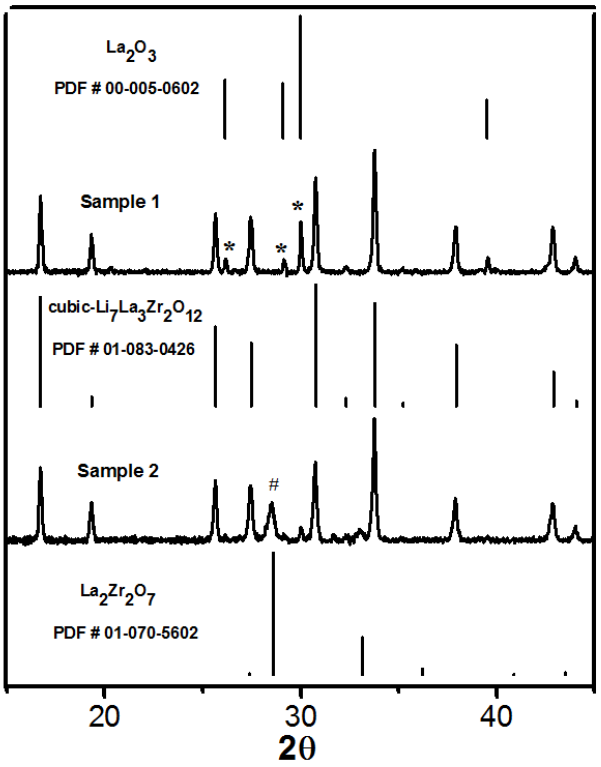

Figure 9. X ray diffraction intensity - 2Θ patterns comparing two similarly treated samples.

It is also worth noting here that this phenomenon only occurs with samples that contain both bismuth and zirconium. That is to say, samples prepared with stoichiometrically correct amount of reagents adhering to the formula $Li_{7-x}La_3Zr_{2-x}Bi_xO_{12}$, as discussed in chapter 3, will form these impurity compounds and they will remain; yet, samples only created to have $Li_7La_3Zr_2O_{12}$ or $Li_5La_3Bi_2O_{12}$ will, with enough heat treatment, form the garnet oxides that is thermodynamically stable. This may be an issue having to do with element specific site occupancy.

CHAPTER 3. COMBINATIONS OF GARNET TYPE OXIDE SYSTEMS

3.1 Phase evolution of mixed complex oxides

By changing the mole ratios of the reagents used in the original synthesis, garnet type oxides of varying stoichiometries can be fabricated through the Pechini method. This modulation in the stoichiometry can be used to adjust for more desirable processing parameters and study effects this modulation can have on material properties such as ionic conductivity. It has already been shown in chapter 2 how there is a difference in phase formation between $Li_7La_3Zr_2O_{12}$ and $Li_5La_3Bi_2O_{12}$ garnet type oxides, but here the changes of compositional variation will be examined.

As there are other figures of merit for this more intricate study, an order of experiments must be established because some of the testing parameters are destructive to the materials being examined. After creation of the pellets, electrodes were painted and cured onto the pellets with conducting silver paint and the pellets were characterized using an impedance analyzer in the frequency range 300000 Hz to 0.0001 Hz. This data would allow for characterization of the lithium-ion transport in through the structure. The Ag paint was polished off before the pellets were fractured and examined with a scanning electron microscope and subsequently tested for density via Archimedes measurements. Finally, the samples were ground and analyzed with powder X-ray diffraction to determine phase composition.

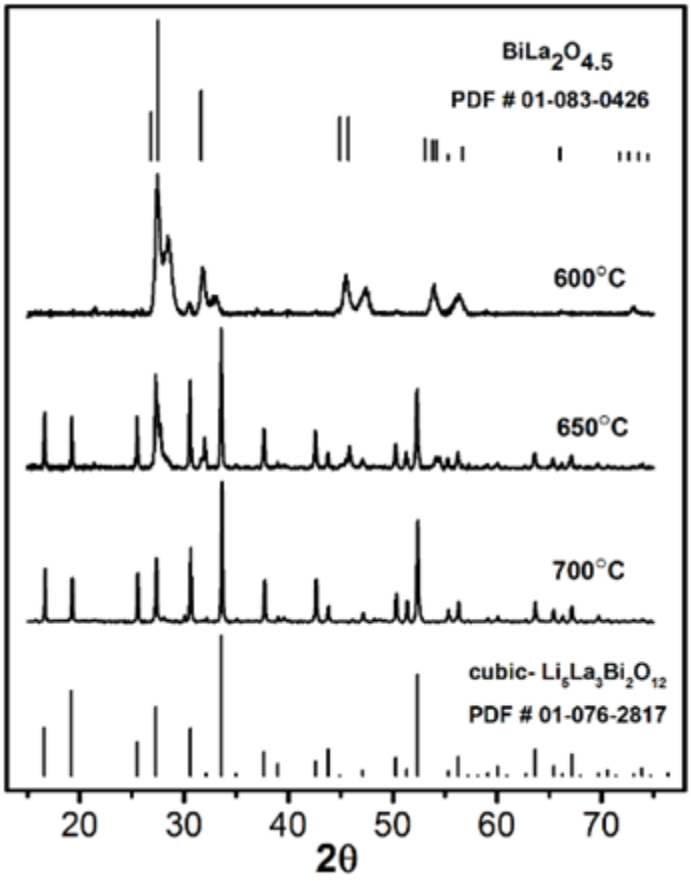

Figure 10. X-ray diffraction intensity - 2Θ patterns for 650 ºC, 700 ºC, and 750 ºC calcination temperatures of polymerized complexes for garnet type oxide $Li_6La_3ZrBiO_{12}$.

Similar to figures 4 and 5, which compare the phase transition of the pure oxide materials, figure 10 shows that the phase transition for calcined mixed oxide polymerized complex. While there is an obvious phase transition before 650 ºC, the transition is not complete as can be seen by the peak trailing around $2\Theta = 28^0$. This reduction in temperature for the cubic phase formation from pure $Li_7La_3Zr_2O_{12}$ implies that the incorporation of bismuth reduces the activation energy required for the phase transformation, even with a 50-50 mixture. Also note that the mixed cubic garnet phase has a lower overall lithium-ion site

occupancy than the because it had fewer ions incorporated to account for the change in valence from zirconium 4+ to bismuth 5+. With less ordering, it can be thus expected to require less thermal activation to achieve the necessary ordering for both the lithium-ion sub-lattice and overall garnet structure.

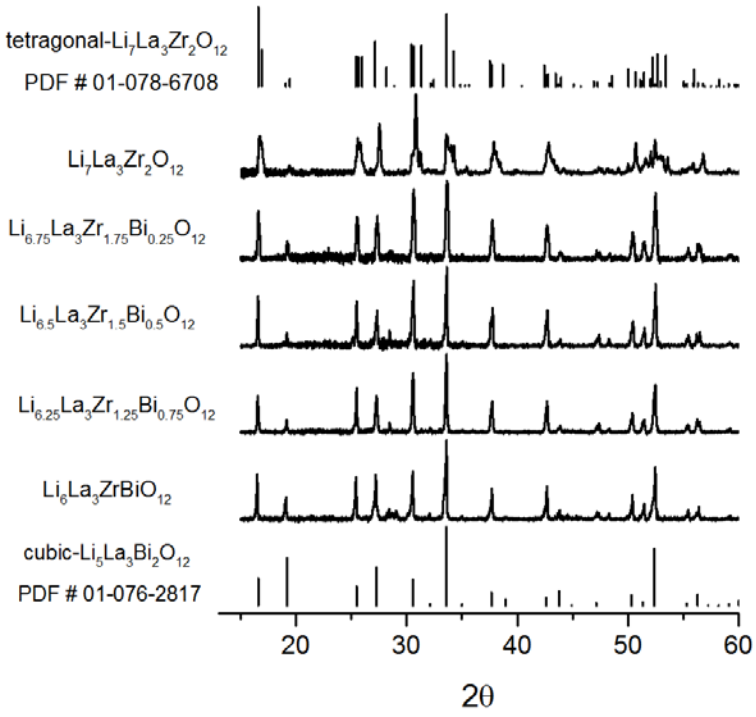

Figure 11. X-ray diffraction intensity - 2Θ patterns for $Li_{7-x}La_3Zr_{2-x}Bi_xO_{12}$ pellets of varying compositions.

To fully understand the role of the bismuth-zirconium tradeoff in both cubic garnet type phase formation and microstructural evolution, pellets of compositions $Li_{7-x}La_3Zr_{2-x}Bi_xO_{12}$ (x = 0, 0.25, 0.5, 0.75, 1.0) sintered at 900 ºC for 10 hours were synthesized and their corresponding diffraction patterns are compared in Figure 11. All samples containing any amount of bismuth are stabilized as cubic Ia-3d phases. In contrast, the $Li_7La_3Zr_2O_{12}$ sample stabilized closer to the I41/acdZ tetragonal phase - with a more ordered lithium-ion sub-lattice, similar to that observed in chapter 2. The stabilization of the cubic phase, even

with a minute amount of bismuth indicates that small quantities of aliovalent dopants preferentially form this more disordered phase at 900 °C. As previously mentioned, this is likely caused by bismuth induced disorder in the lithium-ion sub-lattice, thus providing energetically favorable conditions for the cubic structure to form over the more ordered tetragonal phase, which has closer to full lithium site occupancy.

3.2 Microstructural development for different compositions

Figure 12 presents scanning electron microscope (SEM) images comparing microstructural fracture surfaces for garnet oxide pellets of varying stoichiometry sintered at 900 °C for 10 hours as previously examined. The images correspond to compositions of $Li_{7-x}La_3Zr_{2-x}Bi_xO_{12}$, where x represents increasing amounts of bismuth in the stoichiometry of 0 (12a), 0.5 (12b), 0.75 (12c) and 1.0 (12d). The image 12a, corresponding to the $Li_7La_3Zr_2O_{12}$ pellet, shows very small, sub-micron sized particles and almost no inter-particle coalescence, indicating very little sintering occurring at 900 °C. In contrast, figures 12b, 12c and 12d, with increasing amounts of bismuth respectively, show a significant amount of grain growth and evidence of increased sintering as a consequence of the bismuth additions. When comparing these images, the sample with the highest amount of bismuth (figure 12d) shows enhanced grain growth and a high degree of inter-particle coalescing relative to the 12b and 12c, indicative of sintering at 900 °C. It can therefore be concluded that mixing even small additions of

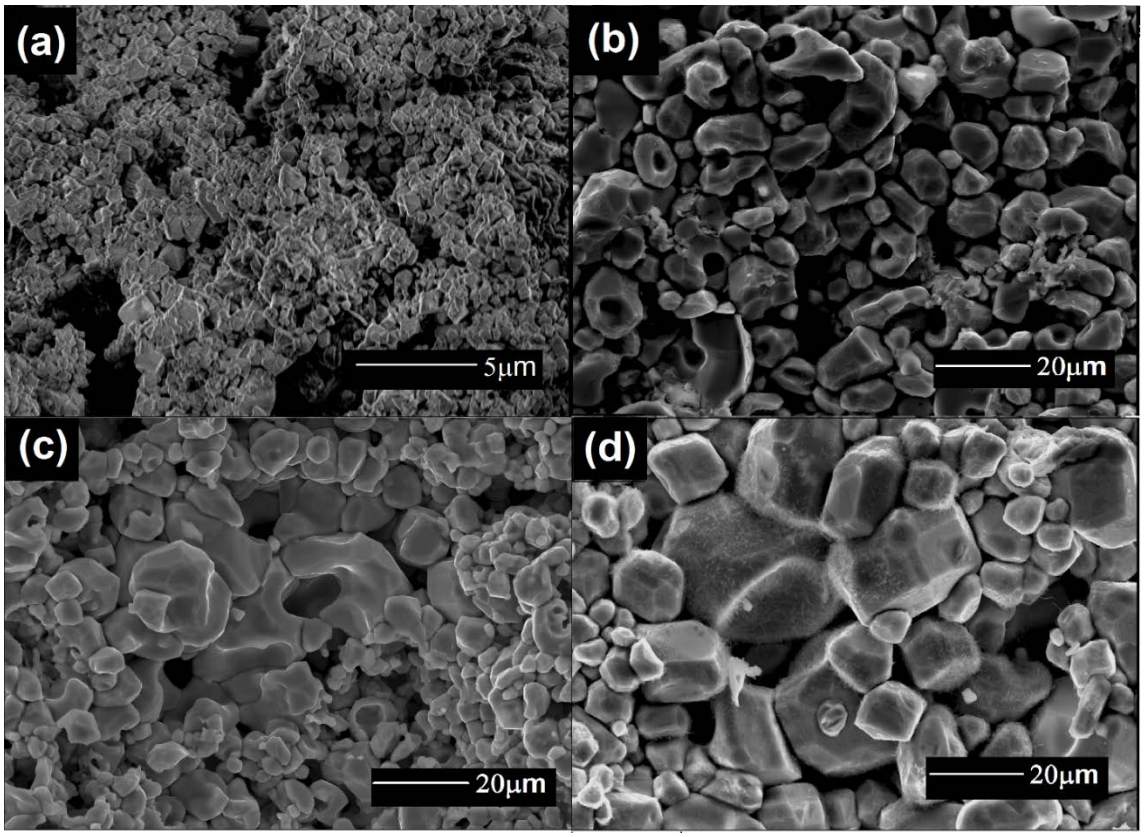

Figure 12. Scanning electron microscope images for $Li_{7-x}La_3Zr_{2-x}Bi_xO_{12}$ fracture surfaces where x = 0 (a), x = 0.5 (b), x – 0.75 (c), and x = 1.0 (d). The images a-d correspond to increasing bismuth concentration.

bismuth in the composition allow to significantly enhance particulate and grain growth and structural interconnectivity. It is not, therefore unreasonable to claim that bismuth acts as a sintering aid and enabler of rapid grain growth; furthermore, the amount of grain growth and densification is correlated to the amount of bismuth added. This remarkable increase may be due to the low eutectic temperatures of some bismuth containing compounds such given that Bi_2O_3 has a melting point of 817 °C. If indeed such low melting eutectic are formed due to bismuth additions at the temperatures utilized in our experiment, even partially, the diffusion velocity and kinetics of crystal growth formation are expected to be

orders or magnitude faster than for the oxide lacking this enabling element. Regardless of the mechanism, there is a significant disparity between the different garnet type complex oxides examined here.

3.3 Materials properties of combined oxides

In an attempt to study the structure-properties relationships of these mixed oxide materials, the ionic conductivity was measured. Figure 13 displays complex impedance plots electrode coated solid electrolyte pellets, which were also examined in figures 11 and 12. Measurements were taken at 27 °C and the plots were analyzed using equivalent circuits models as described by Huggins [62]. As expected, the tail on the low frequency end of the spectra indicates the capacitive nature of the electrodes, while the semicircles at the high frequency end correspond to the resistive-capacitive response of the bulk material. The semicircles at high frequencies are somewhat compressed, indicating separate contributions from both the bulk and grain boundaries, but there is no significant separation. As there is no clear separation between the bulk and grain boundaries, the more resistive nature of the bulk dominates the behavior in comparison to that of the grain boundaries. The compressed semicircles allow for the measurement of the total resistance, as extracted from the low frequency intercept of the Z' axis, as was done studies taking similar measurements [63]. The $Li_7La_3Zr_2O_{12}$ sample did not provide reliable data from which to infer its ionic conductivity. This is likely due to the lack of interconnectivity and low densification present at the 900 °C as indicated in Fig. 12a. In sharp contrast, samples containing bismuth, exhibit considerable grain growth and densification, to provide measurable room temperature ionic conductivity values. The samples yield ionic

conductivity ranging from 10^{-6} – 10^{-4} S/cm and are summarized in Table 1 along with other pellet sample properties.

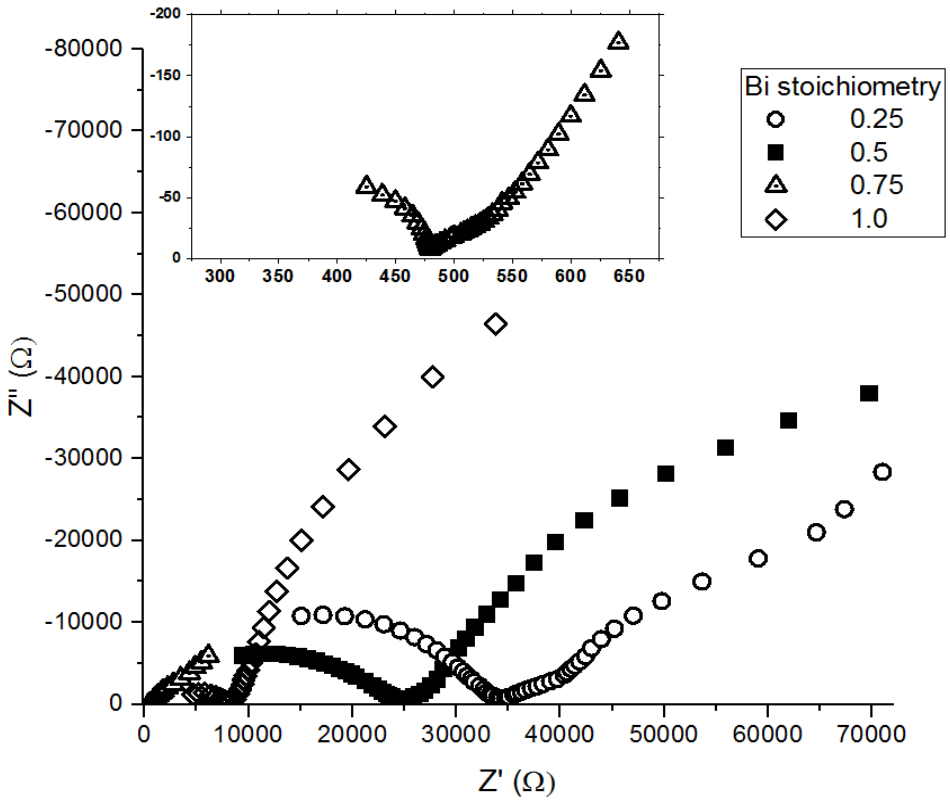

Figure 13. Nyquist plots for $Li_{7-x}La_3Zr_{2-x}Bi_xO_{12}$ samples for Bi stoichiometries of 0.25, 0.5, 0.75, and 1.0.

The trend of higher ionic conductivity with samples containing increasing amounts of bismuth can be partially ascribed to the increments in densification and grain growth attributed to higher bismuth concentrations. The microstructural results provided in figure 12 indicate that increasing amounts of bismuth increase grain growth and sample densification. Moreover, these same samples approach a higher relative density as evidenced by the Archimedes measurements summarized in Table 1. Finally, the increased inter-particle connectivity and coalescence observed in figure 12 results in a lower overall

sample resistance to ionic transport through the densified structure. Thus, samples containing lower amounts of bismuth such as $Li_{6.75}La_3Zr_{1.75}Bi_{0.25}O_{12}$ (x = 0.25) can be expected to have a higher resistance due to larger free volume in the structure.

Table 1. Summary of pellet dimensions and material properties for Bi-doped LLZO pellets sintered at 900 ºC for 10 hours.

Composition	Bi	Thickness (mm)	Density (g/cm^3)	Relative density	Ionic conductivity (S/cm) at 27 □C
$Li_7La_3Zr_2O_{12}$	0	1.51	4.0	0.79	Not measurable
$Li_{6.75}La_3Zr_{1.75}Bi_{0.25}O_{12}$	0.25	1.48	4.2	0.80	5.0×10^{-6}
$Li_{6.5}La_3Zr_{1.5}Bi_{0.5}O_{12}$	0.5	1.30	4.4	0.81	7.2×10^{-6}
$Li_{6.25}La_3Zr_{1.25}Bi_{0.75}O_{12}$	0.75	1.01	4.7	0.83	2.0×10^{-4}
$Li_6La_3ZrBiO_{12}$	1.0	1.08	4.8	0.84	1.2×10^{-5}

In addition to the microstructural aspects, the effect of bismuth inclusion on lithium occupancy needs to be addressed. As the bismuth stoichiometry in the samples is varied, the lithium occupancy to vacancy ratio in the samples proportionally changes, with each bismuth creating an additional lithium vacancy. Thus, it is expected that each pellet composition measured in this study has a different lithium sub-lattice occupancy ratio for the same garnet crystal structure. This variation in stoichiometry causes a change in the electronic structure of these $Li_{7-x}La_3Zr_{2-x}Bi_xO_{12}$ garnets. The composition $Li_{6.25}La_3Zr_{1.25}Bi_{0.75}O_{12}$ (x = 0.75) is observed to have the maximum ionic conductivity in this study; this sample corresponds to a lithium stoichiometry of 6.25, slightly lower than that the typically accepted value of 6.5, which was determined in a compilation of similar studies by Zeier [64]. The difference in these values is likely due to the microstructural and

densification disparities of the samples for varying amounts of bismuth. In comparison to previous studies, samples having comparable densification are fabricated using methods such as hot pressing, thereby making the measured ionic conductivity differences can be directly ascribed to changes in electronic structure [65], [66]. In this experiment we observe significant microstructural and densification dependence on the bismuth composition; indicating that both the densification and lithium occupancy need to be taken into account. For the processing parameters studied here, the tradeoff between lithium site occupancy and densification allows for $Li_{6.25}La_3Zr_{1.25}Bi_{0.75}O_{12}$ to possess the most desirable properties for heat treatment of 900 °C for 10 hours. Other garnet compositions with better properties for even this same system could be achieved through the optimization of heat treatment and stoichiometry.

CHAPTER 4. CONCLUSIONS AND FUTURE WORK

4.1 Conclusions

Crystalline ceramics electrolyte materials such as the garnet type oxides, are typically fabricated employing conventional solid-state reactions relying on mechanical milling and sintering. Solution based synthesis through a polymerized-complex decreases the fabrication temperature required for crystallinity. This Pechini method fabrication of the complex oxides is a successful way to produce ionic conducting ceramics with varying densities, as studied by TGA, XRD, SEM, and impedance spectroscopy. Ultimately, there is a strong correlation between materials structure, processing, and properties as illustrated by studying the combination of $Li_7La_3Zr_2O_{12}$ and $Li_5La_3Bi_2O_{12}$ garnet type structures. Both microstructural changes resulting from sintering and lithium occupancy optimization in the garnet structure influence the ionic conductivity of these materials. As such, garnets oxides require optimized heat treatments for specific stoichiometries to attain the highest ionic conductivity.

4.2 Future work

A significant challenge with this class of materials will be incorporating the correct stoichiometry and microstructure into solid-state batteries through a process that is able to scale with manufacturing. A review of the numerous studies detailing garnet doping and lattice arrangements have suggested that this class of materials is limited by its structural

framework [64]. However, utilizing a rational method to design materials and devices, this structural limitation can be circumvented with the engineering of thinner electrolyte films. Effort should be focused on scalable processes utilizing thin film and solution based fabrication methods as tools for optimizing compositional and morphological components of novel electrolytes as they are incorporated into solid-state batteries via roll-to-roll processing. There is a need for scalable, low temperature processing methods for creation of crystalline ceramic electrolytes, as are discussed here.

Other avenues for future application of this work can deal with the incorporation of these oxide materials into composites. As was discussed, there is often a significant grain boundary resistance to the ionic motion in through the structure, but the bulk of these crystalline materials has good transport properties. If they were to be included in polymer composites that are able to improve the inter-particulate transport, electrolytes could be created which have useful values for ionic conductivity, but still maintain the advantages of a solid state active separator material. Ultimately, the future of this work should focus on producing next generation batteries by leveraging the functionality of the materials and processes.

LIST OF REFERENCES

LIST OF REFERENCES

[1] B. Scrosati, D. Chimica, and R. La, “Lithium Rocking Chair Batteries : An Old Concept ? History of Rocking Chair Batteries,” *J. Electrochem. Soc.*, vol. 139, no. 10, pp. 2776–2781, 1992.

[2] P. . Stallworth, J. . Fontanella, M. . Wintersgill, C. D. Scheidler, J. J. Immel, S. . Greenbaum, and A. . Gozdz, “NMR, DSC and high pressure electrical conductivity studies of liquid and hybrid electrolytes,” *J. Power Sources*, vol. 81–82, pp. 739–747, Sep. 1999.

[3] M. S. Ding, “Electrolytic Conductivity and Glass Transition Temperature as Functions of Salt Content , Solvent Composition , or Temperature for LiPF 6 in Propylene Carbonate + Diethyl Carbonate,” *J. Chem. Eng. Data*, vol. 48, no. 3, pp. 519–528, 2003.

[4] P. Willmann and D. Lemordant, “Modeling viscosity and conductivity of lithium salts in g -butyrolactone,” *J. Power Sources*, vol. 109, pp. 203–213, 2002.

[5] E. Paled, “The Electrochemical Behavior of Alkali and Alkaline Earth Metals in Nonaqueous Battery Systems-- The Solid Electrolyte Interphase Model,” *J. Electrochem. Soc.*, vol. 126, no. 12, pp. 2047–2051, 1979.

[6] O. Crowther and A. C. West, “Effect of Electrolyte Composition on Lithium Dendrite Growth,” *J. Electrochem. Soc.*, vol. 155, no. 11, p. A806, 2008.

[7] D. E. Fenton, J. M. Parker, and P. V. Wright, “Complexes of alkali metal ions with poly(ethylene oxide),” *Polymer (Guildf).*, vol. 14, no. 11, p. 589, Nov. 1973.

[8] M. Armand, “The history of polymer electrolytes,” *Solid State Ionics*, vol. 69, no. 3–4, pp. 309–319, Aug. 1994.

[9] E. A. Rietman, M. L. Kaplan, and R. J. Cava, “Alkalai Metal Ion-Poly(ethyleneoxide) complexes II. Effects of cation on conductivitC,” *Solid State Ionics*, vol. 25, pp. 41–44, 1987

[10] G. S. Macglashan, Y. G. Andreev, and P. G. Bruce, “Structure of the polymer electrolyte poly (ethylene oxide) 6 : LiAsF6,” *Lett. to Nat.*, vol. 398, pp. 792–794, 1999.

[11] K. Hayamizu, S. Tsuzuki, S. Seki, Y. Ohno, H. Miyashiro, and Y. Kobayashi, “Quaternary Ammonium Room-Temperature Ionic Liquid Including an Oxygen Atom in Side Chain/Lithium Salt Binary Electrolytes: Ionic Conductivity and 1 H, 7 Li, and 19 F NMR Studies on Diffusion Coefficients and Local Motions,” *J. Phys. Chem. B*, vol. 112, no. 4, pp. 1189–1197, 2008.

[12] V. G. Tammann and W. Hesse, “Die Abhaengigkeit der Viscositaet von der Temperatur bei unterkuhlten Fluessigkeiten.,” *Zeitschrift fuer Anorg. und algemeine Chemie*, vol. 156, no. 1, pp. 245–257, 1924.

[13] Y. V Baskakova, O. V Yarmolenko, and O. N. Efimov, “Polymer gel electrolytes for lithium batteries,” *Russ. Chem. Rev.*, vol. 81, no. 4, pp. 367–380, Apr. 2012.

[14] A. R. Rodger, J. Kuwano, and A. R. West, “Li-Ion Conducting Solid Solutions in the Systems Li4XO4 - Li3YO4: X = Si, Ge, Ti; Y = P, As, V; Li4XO4 - LiZO2: Z = Al, Ga, Cr AND Li4GeO4 - Li2CaGeO4,” *Solid State Ionics*, vol. 15, pp. 185–198, 1985.

[15] R. Mercier, J.-P. Malugani, B. Fahys, and G. Robert, “Superionic conduction in Li2S - P2S5 - LiI - Glasses,” *Solid State Ionics*, vol. 5, pp. 663–666, 1981.

[16] J. Saienga and S. W. Martin, “The comparative structure, properties, and ionic conductivity of LiI+Li2S+GeS2 glasses doped with Ga2S3 and La2S3,” *J. Non. Cryst. Solids*, vol. 354, no. 14, pp. 1475–1486, Mar. 2008.

[17] J. Rogez, P. Knauth, A. Garnier, H. Ghobarkar, and O. Schaf, “Determination of the crystallization enthalpies of lithium ion conducting alumino - silicate glasses,” *J. Non. Cryst. Solids*, vol. 262, pp. 177–182, 2000.

[18] J. B. Bates, N. J. Dudney, G. R. Gruzalski, R. A. Zuhr, A. Choudhury, and C. F. Luck, “Electrical properties of amorphous lithium electrolyte thin films,” *Solid State Ionics*, vol. 56, pp. 647–654, 1992.

[19] J. B. Bates, N. J. Dudney, G. R. Gruzalski, R. A. Zuhr, A. Choudhury, and C. F. Luck, “Fabrication and characterization of amorphous lithium electrolyte thin films and rechargeable thin-film batteries,” *J. Power Sources*, vol. 43–44, pp. 103–110, 1993.

[20] P. Knauth, “Inorganic solid Li ion conductors: An overview,” *Solid State Ionics*, vol. 180, no. 14–16, pp. 911–916, Jun. 2009.

[21] H. Hong, “Crystal Structure and Ionic Conductivity of Li14Zn(GeO4)4 and other new Li+ Superionic Conductors,” *Mater. Res. Bull.*, vol. 13, pp. 117–124, 1978.

[22] Y. a. Du and N. a. W. Holzwarth, “Li Ion Diffusion Mechanisms in the Crystalline Electrolyte γ-Li[sub 3]PO[sub 4],” *J. Electrochem. Soc.*, vol. 154, no. 11, p. A999, 2007.

[23] R. Kanno, T. Hata, Y. Kawamoto, and M. Irie, “Synthesis of a new lithium ionic conductor , thio-LISICON – lithium germanium sulfide system,” *Solid State Ionics*, vol. 130, pp. 97–104, 2000.

[24] N. Kamaya, K. Homma, Y. Yamakawa, M. Hirayama, R. Kanno, M. Yonemura, T. Kamiyama, Y. Kato, S. Hama, K. Kawamoto, and A. Mitsui, “A lithium superionic conductor.,” *Nat. Mater.*, vol. 10, no. 9, pp. 682–6, Sep. 2011.

[25] H. Aono, E. Sugimoto, Y. Sadaoka, N. Imanaka, and G. Adachi, “Ionic Conductivity of the Lithium Titanium Phosphate (Lil+xMxTi2-x(PO4)3, M = Al, Sc, Y, and La) Systems,” *J. Electrochem. Soc.*, vol. 136, no. 2, pp. 590–591, 1989.

[26] L.-O. Hagman and P. Kierkegaard, “The Crystal Structure of NaMe2IV(PO4)3; MeIV = Ge, Ti, Zr,” *Acta Chem. Scand.*, vol. 22, pp. 1822–1832, 1968.

[27] M. Cretin and P. Fabry, “Comparative Study of Lithium Ion Conductors in the System Li 1 + x Al x A 2 À x IV (PO 4) 3 with A IV = Ti or Ge and 0 x 0 . 7 for Use as Li + Sensitive Membranes,” *J. Eur. Ceram. Soc.*, vol. 19, pp. 2931–2940, 1999.

[28] H. Aono, E. Sugimoto, Y. Sadaoka, N. Imanaka, and G. Adachi, “Electrical property and sinterability of LiTi2 (P04) 3,” *Solid State Ionics*, vol. 47, pp. 257–264, 1991.

[29] Â. A. Alonso, J. Sanz, J. Santamaría, C. Leon, A. Varez, and T. Fernandez-Diaz, “On the Location of Li+ Cations in the Fast Li-Cation Conductor La0.5Li0.5TiO3 Perovskite,” *Angew. Chemie Int. Ed.*, vol. 112, pp. 633–634, 2000.

[30] Y. INAGUMA, L. CHEN, M. ITOH, and T. NAKAMURA, “Candidate compounds with perovskite structure for high lithium ionic conductivity,” *Solid State Ionics*, vol. 70–71, pp. 196–202, May 1994.

[31] S. Stramare, V. Thangadurai, and W. Weppner, “Lithium Lanthanum Titanates: A Review,” *Chem. Mater.*, vol. 15, no. 21, pp. 3974–3990, Oct. 2003.

[32] H. Geng, J. Lan, A. Mei, Y. Lin, and C. W. Nan, “Effect of sintering temperature on microstructure and transport properties of Li3xLa2/3−xTiO3 with different lithium contents,” *Electrochim. Acta*, vol. 56, no. 9, pp. 3406–3414, Mar. 2011.

[33] S. García-Martín, A. Morata-Orrantía, M. a Alario-Franco, J. Rodríguez-Carvajal, and U. Amador, “Beyond the structure-property relationship paradigm: influence of the crystal structure and microstructure on the Li+ conductivity of La2/3Li(x)Ti(1-x)Al(x)O3 Oxides.,” *Chem. - A Eur. J.*, vol. 13, no. 19, pp. 5607–5616, Jan. 2007.

[34] M. Nb, V. Thangadurai, H. Kaack, and W. J. F. Weppner, “Novel Fast Lithium Ion Conduction in Garnet-Type Li 5 La 3 M 2 O 12 (M = Nb, Ta),” *J. Am. Ceram. Soc.*, vol. 86, pp. 437–440, 2003.

[35] V. Thangadurai and W. Weppner, “Li6ALa2Ta2O12 (A = Sr, Ba): Novel Garnet-Like Oxides for Fast Lithium Ion Conduction,” *Adv. Funct. Mater.*, vol. 15, no. 1, pp. 107–112, Jan. 2005.

[36] T. Zaiß, M. Ortner, R. Murugan, and W. Weppner, “Fast ionic conduction in cubic hafnium garnet Li7La3Hf2O12,” *Ionics (Kiel).*, vol. 16, no. 9, pp. 855–858, Oct. 2010.

[37] A. a. Hubaud, D. J. Schroeder, B. Key, B. J. Ingram, F. Dogan, and J. T. Vaughey, “Low temperature stabilization of cubic (Li7−xAlx/3)La3Zr2O12: role of aluminum during formation,” *J. Mater. Chem. A*, vol. 1, no. 31, p. 8813, 2013.

[38] C. a Geiger, E. Alekseev, B. Lazic, M. Fisch, T. Armbruster, R. Langner, M. Fechtelkord, N. Kim, T. Pettke, and W. Weppner, “Crystal chemistry and stability of ‘Li7La3Zr2O12’ garnet: a fast lithium-ion conductor.,” *Inorg. Chem.*, vol. 50, no. 3, pp. 1089–97, Feb. 2011.

[39] Y. Li, J.-T. Han, C.-A. Wang, H. Xie, and J. B. Goodenough, “Optimizing Li+ conductivity in a garnet framework,” *J. Mater. Chem.*, vol. 22, no. 30, pp. 15357–15361, 2012.

[40] S. Ohta, T. Kobayashi, and T. Asaoka, “High lithium ionic conductivity in the garnet-type oxide Li7−X La3(Zr2−X, NbX)O12 (X=0–2),” *J. Power Sources*, vol. 196, no. 6, pp. 3342–3345, Mar. 2011.

[41] Y. Jin and P. J. McGinn, “Li7La3Zr2O12 electrolyte stability in air and fabrication of a Li/Li7La3Zr2O12/Cu0.1V2O5 solid-state battery,” *J. Power Sources*, vol. 239, pp. 326–331, Oct. 2013.

[42] M. Kotobuki and M. Koishi, “Preparation of Li7La3Zr2O12 solid electrolyte via a sol–gel method,” *Ceram. Int.*, vol. 40, no. 3, pp. 5043–5047, Apr. 2014.

[43] H. T. T. Le, R. S. Kalubarme, D. T. Ngo, S.-Y. Jang, K.-N. Jung, K.-H. Shin, and C.-J. Park, “Citrate gel synthesis of aluminum-doped lithium lanthanum titanate solid electrolyte for application in organic-type lithium-oxygen batteries,” *J. Power Sources*, vol. 274, pp. 1188–1199, Oct. 2014.

[44] V. Thangadurai, S. Narayanan, and D. Pinzaru, “Garnet-type solid-state fast Li ion conductors for Li batteries: critical review.,” *Chem. Soc. Rev.*, vol. 43, no. 13, pp. 4714–27, Jul. 2014.

[45] L. J. Miara, S. P. Ong, Y. Mo, W. D. Richards, Y. Park, J. Lee, H. S. Lee, and G. Ceder, “E ff ect of Rb and Ta Doping on the Ionic Conductivity and Stability of the Garnet Li 7+2x-y(La3-xRbx)(Zr2-yTay)O12 (0<x<0.375, 0<y<1) Superionic Conductor: A First Principles Investigation,” *Chemist*, vol. 25, pp. 3048–3055, 2013.

[46] E. J. Cussen, “Structure and ionic conductivity in lithium garnets,” *J. Mater. Chem.*, vol. 20, no. 25, p. 5167, 2010.

[47] E. J. Cussen and T. W. S. Yip, “A neutron diffraction study of the d0 and d10 lithium garnets Li3Nd3W2O12 and Li5La3Sb2O12,” *J. Solid State Chem.*, vol. 180, no. 6, pp. 1832–1839, Jun. 2007.

[48] V. Thangadurai and W. Weppner, “Li6ALa2Nb2O12 (A=Ca, Sr, Ba): A New Class of Fast Lithium Ion Conductors with Garnet-Like Structure,” *J. Am. Ceram. Soc.*, vol. 88, no. 2, pp. 411–418, Feb. 2005.

[49] R. Murugan, V. Thangadurai, and W. Weppner, “Fast Lithium Ion Conduction in Garnet-Type Li7La3Zr2O12,” *Angew. Chemie Int. Ed.*, vol. 46, no. 41, pp. 7778–7781, Oct. 2007.

[50] J. Awaka, A. Takashima, K. Kataoka, N. Kijima, Y. Idemoto, and J. Akimoto, “Crystal Structure of Fast Lithium-ion-conducting Cubic Li7La3Zr2O12,” *Chem. Lett.*, vol. 40, no. 1, pp. 60–62, 2011.

[51] N. Bernstein, M. D. Johannes, and K. Hoang, “Origin of the Structural Phase Transition in Li_{7}La_{3}Zr_{2}O_{12},” *Phys. Rev. Lett.*, vol. 109, no. 20, p. 205702, Nov. 2012.

[52] C. Deviannapoorani, L. Dhivya, S. Ramakumar, and R. Murugan, “Lithium ion transport properties of high conductive tellurium substituted Li7La3Zr2O12 cubic lithium garnets,” *J. Power Sources*, vol. 240, pp. 18–25, Oct. 2013.

[53] L. Dhivya, N. Janani, B. Palanivel, and R. Murugan, “Li+ transport properties of W substituted Li7La3Zr2O12 cubic lithium garnets,” *AIP Adv.*, vol. 3, no. 8, p. 082115, 2013.

[54] R. Murugan, S. Ramakumar, and N. Janani, “High conductive yttrium doped Li7La3Zr2O12 cubic lithium garnet,” *Electrochem. commun.*, vol. 13, no. 12, pp. 1373–1375, Dec. 2011.

[55] M. Huang, A. Dumon, and C.-W. Nan, “Effect of Si, In and Ge doping on high ionic conductivity of Li7La3Zr2O12,” *Electrochem. commun.*, vol. 21, pp. 62–64, Jul. 2012.

[56] J. Wolfenstine, J. Ratchford, E. Rangasamy, J. Sakamoto, and J. L. Allen, “Synthesis and high Li-ion conductivity of Ga-stabilized cubic Li7La3Zr2O12,” *Mater. Chem. Phys.*, vol. 134, no. 2–3, pp. 571–575, Jun. 2012.

[57] J. L. Allen, J. Wolfenstine, E. Rangasamy, and J. Sakamoto, “Effect of substitution (Ta, Al, Ga) on the conductivity of Li7La3Zr2O12,” *J. Power Sources*, vol. 206, pp. 315–319, May 2012.

[58] M. a Howard, O. Clemens, E. Kendrick, K. S. Knight, D. C. Apperley, P. a Anderson, and P. R. Slater, “Effect of Ga incorporation on the structure and Li ion conductivity of La3Zr2Li7O12.,” *Dalton Trans.*, vol. 41, no. 39, pp. 12048–53, Oct. 2012.

[59] H.M. Richenback, P.J. McGinn. “Combanatorial synthesis of oxide powders.,” *J. Mater. Res.*, vol. 16, no. 4, pp. 967–73, Apr. 2001.

[60] I. Kokal, M. Somer, P.H.L. Notten, H.T. Hintzen. “Sol-gel synthesis and lithum ion conductivity of La7La3Zr2O12 with garnet-related type structure.,” *Solid State Ionics.*, vol. 185, pp. 43-6, Oct. 2014.

[61] Y. X. Gao, X. P. Wang, W. G. Wang, Z. Zhuang, D. M. Zhang, and Q. F. Fang, “Synthesis, ionic conductivity, and chemical compatibility of garnet-like lithium ionic conductor Li5La3Bi2O12,” *Solid State Ionics*, vol. 181, no. 31–32, pp. 1415–1419, Oct. 2010.

[62] R. A. Huggins, “Simple Method to Determine Electronic and Ionic Components of the Conductivity in Mixed Conductors A Review,” *Ionics (Kiel).*, vol. 8, no. 3–4, pp. 300–313, 2002.

[63] J. Wolfenstine, E. Rangasamy, J. L. Allen, and J. Sakamoto, “High conductivity of dense tetragonal Li7La3Zr2O12,” *J. Power Sources*, vol. 208, pp. 193–196, Jun. 2012.

[64] W. G. Zeier, “Structural limitations for optimizing garnet-type solid electrolytes: a perspective.,” *Dalton Trans.*, vol. 43, no. 43, pp. 16133–8, Oct. 2014.

[65] J. L. Allen, J. Wolfenstine, E. Rangasamy, and J. Sakamoto, “Effect of substitution (Ta, Al, Ga) on the conductivity of Li7La3Zr2O12,” *J. Power Sources*, vol. 206, pp. 315–319, May 2012.

[66] E. Rangasamy, J. Wolfenstine, and J. Sakamoto, “The role of Al and Li concentration on the formation of cubic garnet solid electrolyte of nominal composition Li3Zr2O12,” *Solid State Ionics*, vol. 206, pp. 28–32, Jan. 2012.